

Mode tuning of photonic crystal nanocavities by photoinduced non-thermal oxidation

Citation for published version (APA):

Intonti, F., Caselli, N., Vignolini, S., Riboli, F., Kumar, S., Rastelli, A., Schmidt, O. G., Francardi, M., Gerardino, A., Balet, L. P., Li, L. H., Fiore, A., & Gurioli, M. (2012). Mode tuning of photonic crystal nanocavities by photoinduced non-thermal oxidation. *Applied Physics Letters*, 100(3), 1-4. Article 033116. <https://doi.org/10.1063/1.3678036>

DOI:

[10.1063/1.3678036](https://doi.org/10.1063/1.3678036)

Document status and date:

Published: 01/01/2012

Document Version:

Publisher's PDF, also known as Version of Record (includes final page, issue and volume numbers)

Please check the document version of this publication:

- A submitted manuscript is the version of the article upon submission and before peer-review. There can be important differences between the submitted version and the official published version of record. People interested in the research are advised to contact the author for the final version of the publication, or visit the DOI to the publisher's website.
- The final author version and the galley proof are versions of the publication after peer review.
- The final published version features the final layout of the paper including the volume, issue and page numbers.

[Link to publication](#)

General rights

Copyright and moral rights for the publications made accessible in the public portal are retained by the authors and/or other copyright owners and it is a condition of accessing publications that users recognise and abide by the legal requirements associated with these rights.

- Users may download and print one copy of any publication from the public portal for the purpose of private study or research.
- You may not further distribute the material or use it for any profit-making activity or commercial gain
- You may freely distribute the URL identifying the publication in the public portal.

If the publication is distributed under the terms of Article 25fa of the Dutch Copyright Act, indicated by the "Taverne" license above, please follow below link for the End User Agreement:

www.tue.nl/taverne

Take down policy

If you believe that this document breaches copyright please contact us at:

openaccess@tue.nl

providing details and we will investigate your claim.

Mode tuning of photonic crystal nanocavities by photoinduced non-thermal oxidation

Francesca Intonti, Niccolò Caselli, Silvia Vignolini, Francesco Riboli, Santosh Kumar et al.

Citation: *Appl. Phys. Lett.* **100**, 033116 (2012); doi: 10.1063/1.3678036

View online: <http://dx.doi.org/10.1063/1.3678036>

View Table of Contents: <http://apl.aip.org/resource/1/APPLAB/v100/i3>

Published by the [American Institute of Physics](http://www.aip.org).

Related Articles

High-Q aluminum nitride photonic crystal nanobeam cavities

Appl. Phys. Lett. **100**, 091105 (2012)

Magnetophotonic crystal comprising electro-optical layer for controlling helicity of light

J. Appl. Phys. **111**, 07A913 (2012)

Multimodal strong coupling of photonic crystal cavities of dissimilar size

Appl. Phys. Lett. **100**, 081107 (2012)

Highly modified spontaneous emissions in YVO₄:Eu³⁺ inverse opal and refractive index sensing application

Appl. Phys. Lett. **100**, 081104 (2012)

High quality factor two dimensional GaN photonic crystal cavity membranes grown on silicon substrate

Appl. Phys. Lett. **100**, 071103 (2012)

Additional information on *Appl. Phys. Lett.*


Journal Homepage: <http://apl.aip.org/>

Journal Information: http://apl.aip.org/about/about_the_journal

Top downloads: http://apl.aip.org/features/most_downloaded

Information for Authors: <http://apl.aip.org/authors>

ADVERTISEMENT



LakeShore Model 8404 developed with **TOYO Corporation**
NEW AC/DC Hall Effect System Measure mobilities down to 0.001 cm²/V s

Mode tuning of photonic crystal nanocavities by photoinduced non-thermal oxidation

Francesca Intonti,^{1,a)} Niccolò Caselli,¹ Silvia Vignolini,¹ Francesco Riboli,¹ Santosh Kumar,² Armando Rastelli,² Oliver G. Schmidt,² Marco Francardi,³ Annamaria Gerardino,³ Laurent Balet,⁴ Lianhe H. Li,⁴ Andrea Fiore,⁵ and Massimo Gurioli¹

¹*LENS and Department of Physics, University of Florence, Via Sansone 1, 50019 Sesto Fiorentino, Italy*

²*Institute for Integrative Nanosciences, IFW Dresden, Helmholtzstr. 20, 01069 Dresden, Germany*

³*Institute of Photonics and Nanotechnology, CNR, 00156 Roma, Italy*

⁴*Ecole Polytechnique Fédérale de Lausanne, Institute of Photonics and Quantum Electronics, CH-1015 Lausanne, Switzerland*

⁵*COBRA Research Institute, Eindhoven University of Technology, 5600 MB Eindhoven, The Netherlands*

(Received 23 September 2011; accepted 22 December 2011; published online 20 January 2012)

A method to achieve photoinduced tuning of PhC nanocavity modes is discussed and implemented. It is based on light induced oxidation in air atmosphere with very low thermal budget which produces a local reduction of the GaAs membrane effective thickness and a large blueshift of the nanocavity modes. It is also shown that green light is much more efficient in inducing the micro-oxidation with respect to near infrared light. The observed behaviour is attributed to oxide growth promoted by photoenhanced reactivity. © 2012 American Institute of Physics. [doi:10.1063/1.3678036]

Photonic crystal (PhC) nanocavities are the building blocks of many advanced optical,^{1,2} optoelectronic,³ and quantum optics devices.^{4,5} For most of these applications, a fundamental requisite is the design and control of the PhC nanocavity modes at the target wavelengths, within an accuracy which is not directly obtainable due to the fabrication tolerances. Different postfabrication processing methods, able to tune the nanocavity modes for compensating the fabrication imperfections, have been therefore demonstrated in the last few years, such as tip⁶ and thermal tuning,^{7,8} wet chemical digital etching,⁹ atomic layer deposition,¹⁰ nano-oxidation,¹¹ liquid nano-infiltration,¹² and nano-electromechanical-structures.^{13,14} Recently, a very simple method based on the thermal oxidation by laser irradiation in air atmosphere has been realized in GaAs,¹⁵ Si,¹⁶ and GaP structures.¹⁷ This method has the great advantage of being local without needing extra materials and processing tools. However, it requires a large thermal budget which can produce undesired annealing and modification of the underlying semiconductor layers.

In this letter, we describe a method to achieve local photoinduced tuning of PhC nanocavity modes with very low thermal budget. It is based on micro-oxidation produced by low power, continuous wave laser micro-irradiation of single nanocavities in air atmosphere. The modes can be largely and smoothly blueshifted due to the local reduction of the GaAs membrane effective thickness after the micro-oxidation. We directly measure the sample temperature during the oxidation by using the PhC modes as a local thermometer, and we extract a temperature rise as low as $T < 47^\circ\text{C}$, in agreement with simulations based on finite element method (FEM) and finite-difference time-domain (FDTD) method. We also show that green light is much

more efficient in inducing the micro-oxidation with respect to near infrared light. This behaviour is attributed to oxide growth promoted by photo enhanced reactivity.

The samples under consideration are 2D PhC microcavities (triangular lattice of air holes with lattice parameter $a = 311\text{ nm}$ and filling fraction $f = 35\%$) of a GaAs based heterostructure. Three layers of high-density InAs quantum dots (QDs) emitting at 1300 nm (acting as integrated light sources) are grown by molecular beam epitaxy at the center of a 320-nm -thick GaAs membrane obtained by selective etching of an AlGaAs sacrificial layer. The nanocavity is formed by four missing holes organized in a diamond-like geometry (denominated D2 cavity). The first two modes of the D2 cavity (hereafter labelled M1 and M2) are spatially extended along the two orthogonal diagonals of the D2 rhomb, and have different polarization properties.⁶ Photoluminescence (PL) spectra of the samples were collected in a confocal configuration using a $50\times$ microscope objective ($\text{NA} = 0.7$). The sample is excited either with light from a diode laser ($\lambda = 780\text{ nm}$) or by an Ar^+ ion laser ($\lambda = 514\text{ nm}$), and the emitted PL signal is coupled to a single-mode optical fiber of $6\ \mu\text{m}$ core diameter, acting as a confocal pinhole, connected to a spectrometer. The PL signal, dispersed by the spectrometer, is finally collected by a liquid nitrogen cooled InGaAs array. The sample is mounted on a XY stage so that it can be scanned in respect to the objective, allowing the collection of two-dimensional PL maps. In order to quantify our spatial resolution, we report in Fig. 1(a) the PL intensity map of the fundamental mode M1 at low excitation power ($P = 0.1\text{ mW}$), where heating can be neglected. The data lead to an estimate of the laser spot of the order of $1.1\ \mu\text{m}$ full width at half maximum. The spectral resolution of the experimental setup is 0.5 nm .

In order to control the local temperature of the samples under laser exposure, we take advantage of the thermal red shift of the photonic modes which, around room temperature,

^{a)} Author to whom correspondence should be addressed. Electronic mail: intonti@lens.unifi.it.

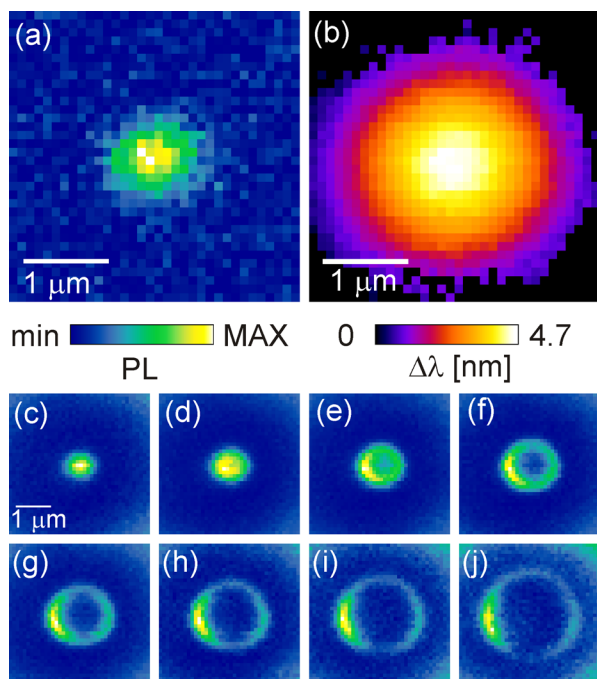


FIG. 1. (Color online) (a) Spatial distribution of the PL signal associated with the M1 mode at low power ($P=0.1$ mW). (b) Map of the temperature gradient obtained with high excitation density. ($P=2.7$ mW). It faithfully describes the laser induced heating using the M1 resonance as a local thermometer, as is more evident from the monochromatic PL maps reported at 0.5 nm steps from the highest wavelength (c) to the lowest (j).

has been calibrated to be 0.12 nm/K.¹⁸ Typical results are reported in Figs. 1(b)–1(j) for excitation at $\lambda=780$ nm, and they refer to the highest excitation power ($P=2.7$ mW) used in the experiment, where a 4.7 nm red shift of the modes at the center of the laser spot can be monitored. In principle, during laser exposure, the modes may shift due to (1) oxidation, (2) optical Kerr effect, (3) free carrier injection, and (4) heating. Oxidation leads to an irreversible blue shift which is negligible for the experimental time exposure corresponding to the data reported in Fig. 1. Optical Kerr effect occurs at much higher excitation power, due to the small non-linearity of GaAs.¹⁹ Optical tuning due to free carrier injection has been studied in Ref. 20; it gives a blue shift and by using the parameter given in Ref. 20, we estimate a blue shift of the order of 1 nm for the data reported in Fig. 1. Heating gives a red shift of the modes and our findings, therefore, demonstrated that it is the dominant effect in our experimental condition. Still the correction for the blue shift (of the order of 20% of the experimental red shift) due to free carrier injection has to be accounted for an accurate estimation of the sample temperature.

The spectral shift map shown in Fig. 1(b) was obtained by spatially scanning the sample under the fixed laser beam and measuring the peak wavelength of the fundamental PhC mode M1 for each position. The map shows that the thermal gradient extends over a 2 μm region, which is slightly larger than the excitation spot. In fact, the PhC mode acts as a local thermometer, and the monochromatic spatial maps, obtained by reporting the PL intensity maps at a given wavelength, can be used to get precise information of the temperature distribution. This is clearly demonstrated by the maps shown in Figs. 1(c)–1(j) at $\Delta\lambda=0.5$ nm steps, so that a local and direct

measurement of the laser induced sample heating can be monitored. The experimental spectral shift of the fundamental mode M1 at the center of the spot is $\Delta\lambda=4.7$ nm, corresponding (including the estimated blue shift for carrier injection) to an increase of temperature of the order of 47 °C [Fig. 1(b)]. The temperature increase is large enough to be carefully measured but extremely low for thermal effects such as annealing or thermal oxidation to be activated. Data for green light from the Ar⁺ laser are very similar; at the maximum power used ($P=0.7$ mW), we observe a temperature increase of $\Delta T=22$ °C.

In order to verify that our data reflect the real temperature of the sample, we use FEM to estimate the laser heating for the realistic structure in the experimental conditions. The temperature profile during laser irradiation is calculated by solving the heat conduction equation, taking into account the temperature-dependent thermal conductivity of bulk GaAs and the power lost due to reflection at the top surface of the membrane. We note that the actual thermal conductivity in the PhC region may be lower than the bulk values due to phonon scattering at the etched interfaces. Heat losses due to convection and conduction in air are neglected. Multiple reflections inside the membrane are also not considered; for green light, the absorption in a single pass through the membrane is more than 90%, and therefore, the approximation is valid. The spatial profile of the calculated temperature at the top surface of the PhC nanocavity at a laser power $P=0.7$ mW and $\lambda=516$ nm (because of the availability of the parameters required for the calculation) is reported in Fig. 2. The temperature reaches its maximum value $\Delta T=16$ °C at the center of the laser spot and drops while moving away from it; thus, experimental data and theoretical simulations nicely fit together. In the case of infrared light, assuming an excitation power of 2.7 mW and $\lambda=780$ nm, the simulation gives at the center of the laser spot a maximum heating of 21 °C. The simulated heating with excitation at $\lambda=780$ nm is underestimated, because the single pass absorption in the membrane is only 38% and neglecting the multiple reflection is likely to be incorrect. Nevertheless, the reliability of the temperature estimation and the very low thermal budget used in our experimental condition are supported by FEM

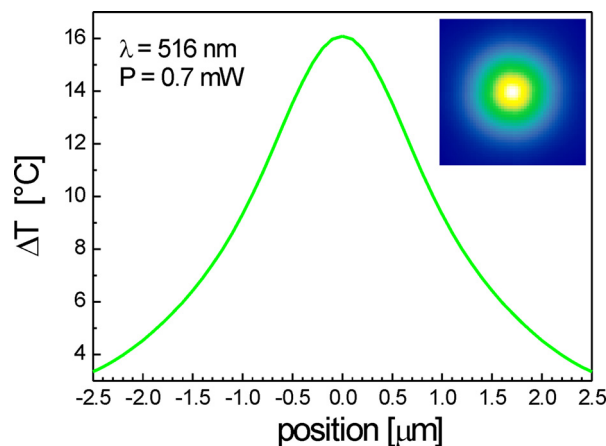


FIG. 2. (Color online) Spatial profile of the calculated temperature gradient at the top surface of the PhC nanocavity at a laser irradiation power of 0.7 mW ($\lambda=516$ nm) obtained with FEM simulation. The inset represents the calculated spatial 2D map ($5 \times 5 \mu\text{m}^2$) of the temperature gradient.

simulations. Also the spatial profile of the FEM temperature map nicely agrees with the experimental data, giving a thermal distribution extending over $2\ \mu\text{m}$.

Despite the very low thermal budget of our exposure condition, we observe that a non reversible modification of the PhC nanocavity occurs after laser illumination of about half an hour under high excitation power, that is, $P = 2.7\ \text{mW}$ for $\lambda = 780\ \text{nm}$ and $P = 0.7\ \text{mW}$ for $\lambda = 514\ \text{nm}$. In fact, when reducing the laser power and after waiting for the cooling of the sample, we observed that the PhC modes undergo sizeable blue shift. The mode shift can be controlled either by varying the laser power or by iterating laser exposure steps. Figure 3(a) displays PL spectra acquired at low power after different exposure times to a high power green laser, showing a large blue shift of the main two resonances without remarkable Q-factor or intensity variations. Data for both excitation wavelengths for mode M1 are given in Fig. 3(b). Although we had larger heating power and correspondingly larger temperature rise in the experiment with infrared excitation, the results clearly indicate that the rate of blue shift is much larger when using the green light. These findings denote a relevant wavelength dependence of the effect.

The time evolution of the irreversible effect is a key aspect to assess its origin. Clearly from the data of Fig. 3(a), the blue shift is not linear with the laser exposure time. A nice linear trend is instead obtained if the data are plotted vs. the square root of the time, as done in Fig. 3(b). This is a fingerprint of a diffusive process. The data presented so far and the similarity with the results of Ref. 15 suggest us to attribute the progressive mode shift with irradiation time to a non-thermal oxidation of the GaAs membrane. The oxidation acts by reducing the membrane effective thickness and/or by increasing the effective photonic pores diameters. In both

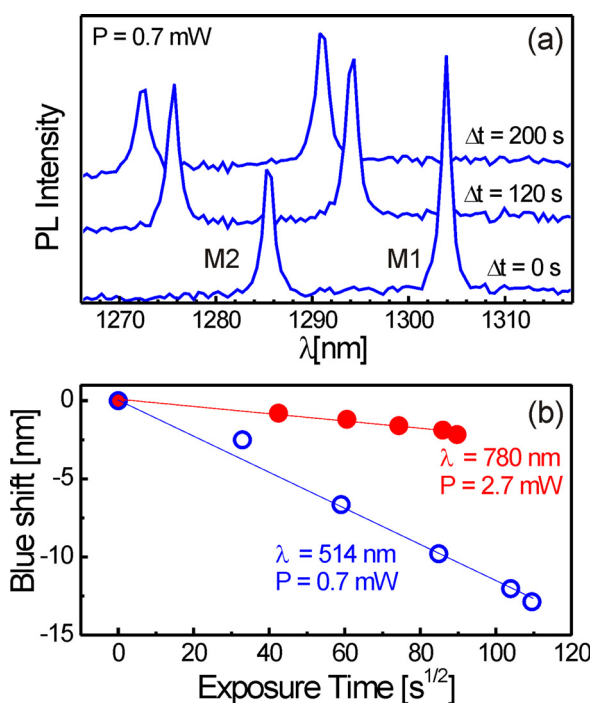


FIG. 3. (Color online) (a) PL spectra of the PhC nanocavity acquired at low power after different exposition times to a high power green laser ($P = 0.7\ \text{mW}$). (b) M1 blue shift data plotted vs. the square root of the time for both excitation wavelengths.

cases, the effect on the photonic mode is a shift toward smaller wavelengths. In order to demonstrate that the blue shift depends on the presence of oxygen in the environment of the sample during laser irradiation, we performed the same experiment in a controlled nitrogen atmosphere. In this case, the blue shift of the PhC modes is missing, indicating that oxygen is requisite for observing the PhC modes spectral shift.

It is well known that the local GaAs oxidation produces oxide protrusions due to the larger molar volume of the oxide with respect to the GaAs. An AFM image of the D2 cavity after a laser exposure corresponding to an overall shift of $13\ \text{nm}$ of the photonic modes is shown in Fig. 4(a). The presence of an oxide protrusion in a spatial region corresponding to the laser spot is clearly observed on the sample. The line scan from left to right is displayed in Fig. 4(b) to depict the height of the oxidized area; a value of about $20\ \text{nm}$ height is found with respect to the non oxidized region. This data could in principle be used to estimate the structural changes of the membrane. From the ratio of the molar volume of stoichiometric oxide (Ref. 21), we expect a reduction of the membrane thickness of the order of $10\ \text{nm}$ on the top interface, and this could be used for calculating the mode shift. However, several important data are missing. First, the oxide can grow also in the bottom side of the membrane and/or in the pores. Second, the oxide can be non-stoichiometric. In Ref. 15, it was assumed that, under thermal oxidation, the oxide would grow isotropically on all the photonic surfaces

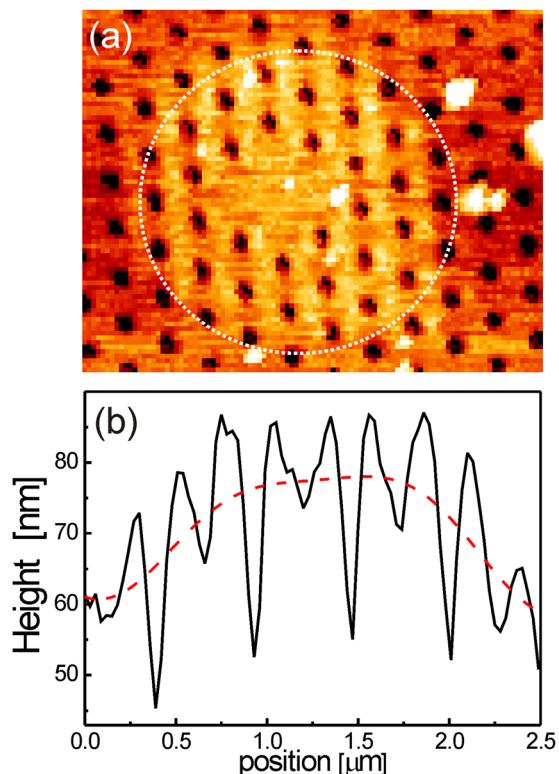


FIG. 4. (Color online) (a) Topography image ($2.5 \times 2.0\ \mu\text{m}^2$) of the D2 cavity after a laser exposure corresponding to an overall shift of $13\ \text{nm}$ of the photonic modes; a protrusion is observed inside the dotted circle due to the laser spot local oxidation. (b) Line profile of (a) allows to evaluate the height of the oxidized region being approximately $20\ \text{nm}$. The red dashed line is a guide to the eyes obtained through a FFT low pass filter.

and this led, from a fit of the mode shift, to a very thin (less than 1 nm) non-stoichiometric oxide protrusion. The morphological data reported here suggest instead the formation of a thick stoichiometric oxide layer (even if the study of the oxide composition is outside the scope of the paper). We performed FDTD (not shown here) simulations in order to link the oxidation to the mode blue shift. We found that the 10 nm membrane-thickness reduction (with the hypothesis of stoichiometric oxide) is too small for accounting the blue shift of the photonic modes of about 13 nm. This finding points out the role of the oxidation of the bottom interface and/or of the pores for a quantitative analysis of the blue shift.

The final point of our analysis is to address the physical mechanisms for explaining the laser assisted non-thermal oxidation of the GaAs. Effects on the GaAs surface after light illuminations have been reported in literature.^{22–25} It has been experimentally observed an excitation-enhanced oxidation of the GaAs surfaces that takes place when the energy of the incident radiation is larger than the GaAs band gap.²² This indicates that a carrier generation at the crystal surface is essential to observe the enhanced oxidation effect. Thus, the photogenerated electron-holes pairs can catalytically enhance the breaking of the substrate bonds²³ and the dissociation of the adsorbate molecules.²⁴ The experimental evidence that the reaction rate per incident photon is strongly dependent on photon energy has been already observed and related to the interaction of hot electrons with O₂ via resonant tunneling.²⁵ It is also important to compare our data with the findings of Ref. 15. The use of higher power with a larger laser spot led to a very different thermal budget (higher temperatures during irradiation). We expect, however, that also in those experiments radiation-enhanced oxidation may have played a role (note the relatively low activation energy value reported in Ref. 15).

In conclusion, the catalytic effect of electron-hole pairs photo-generated at the surface of PhC nanocavities produces a large and fine controlled tuning of the resonances without drastically increasing the sample temperature. The laser assisted oxidation of the sample determines a local modification of the nanocavities, reducing the effective membrane thickness and increasing the effective photonic pores diameter. Post growth local control of the photonic modes with a low thermal budget that avoids annealing and/or damage of the quantum emitters (such as quantum wells or quantum dots) can be exploited also for changing on demand the coupling strength between emitters and optical modes or

between different modes in systems with two or more PhC nanocavities.

The authors thank V. Matarrazzo for helping in the sample holder development. This work was financially supported by the MIUR project PRIN2008H9ZAZR.

- ¹T. Tanabe, M. Notomi, S. Mitsugi, A. Shinya, and E. Kuramochi, *Appl. Phys. Lett.* **87**, 151112 (2005).
- ²B. S. Song, S. Noda, and T. Asano, *Science* **300**, 1537 (2003).
- ³M. Lončar, T. Yoshie, A. Scherer, P. Gogna, and Y. Qiu, *Appl. Phys. Lett.* **81**, 2680 (2002).
- ⁴T. Yoshie, A. Scherer, J. Hendrickson, G. Khitrova, H. M. Gibbs, G. Rupper, C. Ell, O. B. Shchekin, and D. G. Deppe, *Nature (London)* **432**, 200 (2004).
- ⁵K. Hennessy, A. Badolato, M. Winger, D. Gerace, M. Atatüre, S. Gulde, S. Fält, E. L. Hu, and A. Imamoglu, *Nature (London)* **445**, 896 (2007).
- ⁶F. Intonti, S. Vignolini, F. Riboli, A. Vinattieri, D. S. Wiersma, M. Colocci, L. Balet, C. Monat, C. Zinoni, L. H. Li *et al.*, *Phys. Rev. B* **78**, 041401(R) (2008).
- ⁷A. Faraon and J. Vučković, *Appl. Phys. Lett.* **95**, 043102 (2009).
- ⁸S. Vignolini, F. Intonti, L. Balet, M. Zani, F. Riboli, A. Vinattieri, D. S. Wiersma, M. Colocci, C. Monat, C. Zinoni *et al.*, *Appl. Phys. Lett.* **93**, 023124 (2008).
- ⁹K. Hennessy, A. Badolato, A. Tamboli, P. M. Petroff, E. Hu, M. Atatüre, J. Dreiser, and A. Imamoglu, *Appl. Phys. Lett.* **87**, 021108 (2005).
- ¹⁰X. Yang, C. J. Chen, C. A. Husko, and C. W. Wong, *Appl. Phys. Lett.* **91**, 161114 (2007).
- ¹¹K. Hennessy, C. Högerle, E. Hu, A. Badolato, and A. Imamoglu, *Appl. Phys. Lett.* **89**, 041118 (2006).
- ¹²F. Intonti, S. Vignolini, F. Riboli, M. Zani, D. S. Wiersma, L. Balet, L. H. Li, M. Francardi, A. Gerardino, A. Fiore *et al.*, *Appl. Phys. Lett.* **95**, 173112 (2009).
- ¹³L. Midolo, P. J. van Veldhoven, M. A. Dünder, R. Nötzel, and A. Fiore, *Appl. Phys. Lett.* **98**, 211120 (2011).
- ¹⁴R. Perahia, J. D. Cohen, S. Meenehan, T. P. M. Alegre, and O. Painter, *Appl. Phys. Lett.* **97**, 191112 (2010).
- ¹⁵H. S. Lee, S. Kiravittaya, S. Kumar, J. D. Plumhof, L. Balet, L. H. Li, M. Francardi, A. Gerardino, A. Fiore, A. Rastelli *et al.*, *Appl. Phys. Lett.* **95**, 191109 (2009).
- ¹⁶C. J. Chen, J. J. Zheng, T. Y. Gu, J. F. McMillan, M. B. Yu, G. Q. Lo, D. L. Kwong, and C. W. Wong, *Opt. Express* **19**, 12480 (2011).
- ¹⁷J. Wolters, A. W. Schell, G. Kewes, N. Nüsse, M. Schoengen, H. Döscher, T. Hannappel, B. Löchel, M. Barth, and O. Benson, *Appl. Phys. Lett.* **97**, 141108 (2010).
- ¹⁸S. Vignolini, F. Intonti, L. Balet, M. Zani, F. Riboli, A. Vinattieri, D. S. Wiersma, M. Colocci, L. H. Li, M. Francardi *et al.*, *Appl. Phys. Lett.* **93**, 023124 (2008).
- ¹⁹A. de Rossi, M. Lauritano, S. Combric, Q. V. Tran, and C. Husko, *Phys. Rev. A* **79**, 043818 (2009).
- ²⁰I. Fushman, E. Waks, D. Englund, N. Stoltz, P. Petroff, and J. Vuckovic, *Appl. Phys. Lett.* **90**, 091118 (2007).
- ²¹C. H. Tsai, S. R. Jian, and H. C. Wen, *Appl. Surf. Sci.* **254**, 1357 (2007).
- ²²T. Suzuki and M. Ogawa, *Appl. Phys. Lett.* **31**, 473 (1977).
- ²³V. M. Bermudez, *J. Appl. Phys.* **54**, 6795 (1983).
- ²⁴S. G. Anderson, Y. Chen, J. M. Seo, and J. H. Weaver, *Phys. Rev. B* **43**, 9621 (1991).
- ²⁵Y. Chen, J. M. Seo, F. Stepniak, and J. H. Weaver, *J. Chem. Phys.* **95**, 8442 (1991).